



Integrated Arctic Observation System

Research and Innovation Action under EC Horizon2020
Grant Agreement no. 727890

Project coordinator:
Nansen Environmental and Remote Sensing Center, Norway

Deliverable 6.1

Climate model initialization: first report on the added value of using data from INTAROS

Start date of project:	01 December 2016	Duration:	60 months
Due date of deliverable:	31 May 2020	Actual submission date:	25 May 2020
Lead beneficiary for preparing the deliverable:	BSC		
Person-months used to produce deliverable:	19.4 pm		


Authors:

Juan C. Acosta Navarro (BSC, lead), Tim Kruschke (SMHI), David Gustafsson (SMHI), Ralf Döscher (SMHI), François Counillon (NERSC), Yongqi Gao (NERSC) and Vladimir Lapin (BSC)

Reviewer:

Pablo Ortega (BSC)

Version	DATE	CHANGE RECORDS	LEAD AUTHOR
1.0	21/05/2020	First complete draft	Juan Acosta Navarro
1.1	22/05/2020	Reviewed	Pablo Ortega
1.2	25/05/2020	Version including addressed reviewer's comments	Juan Acosta Navarro
1.3	26/05/2020	Final version including addressed PM comments	Juan Acosta Navarro
1.4	29/05/2020	Technical review and submission	Kjetil Lygre

Approval	Date:	Sign.
X	29 May 2020	 Coordinator

USED PERSON-MONTHS FOR THIS DELIVERABLE					
No	Beneficiary	PM	No	Beneficiary	PM
1	NERSC	6	24	TDUE	
2	UiB		25	GINR	
3	IMR		26	UNEXE	
4	MISU		27	NIVA	
5	AWI		28	CNRS	
6	IOPAN		29	U Helsinki	
7	DTU		30	GFZ	
8	AU		31	ARMINE	
9	GEUS		32	IGPAN	
10	FMI		33	U SLASKI	
11	UNIS		34	BSC	7
12	NORDECO		35	DNV GL	
13	SMHI	6.4	36	RIHMI-WDC	
14	USFD		37	NIERSC	
15	NUIM		38	WHOI	
16	IFREMER		39	SIO	
17	MPG		40	UAF	
18	EUROGOOS		41	U Laval	
19	EUROCEAN		42	ONC	
20	UPM		43	NMEFC	
21	UB		44	RADI	
22	UHAM		45	KOPRI	
23	NORCE		46	NIPR	
			47	PRIC	

DISSEMINATION LEVEL		
PU	Public, fully open	X
CO	Confidential, restricted under conditions set out in Model Grant Agreement	
CI	Classified, information as referred to in Commission Decision 2001/844/EC	

EXECUTIVE SUMMARY

This report describes the first results of the work performed in Task 6.1, that has the main goal of improving the skill of climate predictions, investigating the benefits related to the exploitation of INTAROS data.

In particular, it includes results from seasonal and decadal prediction systems with two different General Circulation Models (NorCPM and EC-Earth), with a central focus on the predictive capacity over the Arctic region. The major goals have been addressed:

- 1) Disentangling the predictability that arises from the initialization of different climate components (sea ice, ocean, hydrology), and the benefits related to the assimilation of specific observational products.
- 2) Quantifying their impact on prediction quality, from the main forecast biases to specific skill metrics

Table of Contents

Introduction	5
INTAROS Data used in this report	6
Benefits of sea-ice thickness initialization for seasonal-to-decadal climate predictions (SMHI contribution)	6
<i>Background and initialization approach</i>	6
<i>Results</i>	7
Impact of sea ice concentration assimilation in seasonal prediction biases (BSC contribution)	10
<i>Summer hindcasts (May initialization)</i>	11
<i>Winter hindcasts (November initialization)</i>	12
Impact of Ocean and Sea Ice Initialisation On Seasonal Prediction Skill in the Arctic (NERSC contribution)	14
<i>Seasonal to decadal predictions of regional Arctic sea ice by assimilating sea surface temperature in the Norwegian Climate Prediction Model</i>	14
<i>Impact of Ocean and Sea Ice Initialisation On Seasonal Prediction Skill in the Arctic</i>	15
<i>Ongoing and Future work:</i>	17
Impact of hydrological observations on prediction of spring floods, river ice breakup and fresh water flow to Arctic Ocean (SMHI contribution)	18
<i>Pan-arctic hydrological model Arctic-HYPE</i>	18
<i>Arctic-HYPE v4.2 OPeNDAP data service</i>	19
<i>Yakutia spring flood and river ice breakup forecasting</i>	20
Conclusions	21
References	22

1. Introduction

Climate predictions aim to estimate the future evolution of climate on sub-seasonal to decadal time scales. Climate predictability stems from two main sources, external forcing and the state of the climate system (ocean, atmosphere, land, cryosphere) prior to the forecast initialization. Forecast systems (i.e. initialized climate models) are essential tools in climate prediction and their correct initialization, which synchronizes the model climate with the real climate, is necessary to exploit the real predictability of the climate system. Knowledge of the climate state at a given point in time is only possible through extensive observations of the different components of the climate system. Furthermore, to correctly evaluate past forecasts and improve the systems, continuous observations in time and space are necessary. This “big picture” view of most of the planet has only been available since satellites became operational in the late 1970s. Additionally, deployment of complementary in-situ observing systems has significantly increased in the past decades, filling important gaps, and as a result improving forecast quality.

The different components of the climate systems interact and have characteristic persistence timescales which together result in predictability. The ocean is the most important component on long timescales (over months to decades), while the atmosphere is critical on short timescales (hours to a week). The land and the sea ice state contain information useful mostly on intermediate timescales (several weeks to over a season). Hence initializing the key variables of the sea ice component may be beneficial for seasonal and decadal predictions, but its correct initialization relies on good observations. Sea ice concentration (SIC) and sea ice thickness (SIT) are thought to be fundamental variables to initialize sea ice in fully coupled models. Arctic-wide SIC observations have been available since the late 1970s, while SIT has become available more recently (early 2000s).

Here we report the initial findings on the impact of INTAROS Arctic products on seasonal and decadal hindcasts with two contemporary forecast systems, EC-Earth and NorCPM. These rely on the use of novel INTAROS observational datasets for the ocean, sea ice and land (the specific sets employed are indicated in Section 2) either for initialization or evaluation, following the workplan established for Task 6.1. Section 3 shows the added value of including SMOS (2010-2020) SIT data in decadal predictions. In section 4, the impact of SIC (CERSAT, 1992-2018) initialization on seasonal forecasts is shown. Finally, Section 5 explains the benefits from initialization of only ocean, and combined ocean and sea ice variables in Arctic sea ice extent seasonal forecasts. In Section 6, we present initial findings of a hydrological use-case where the impact of assimilation of the Arctic-HYCOS hydrological observations (assessed and enhanced within WP2) on monitoring and forecasting of spring flood, river ice breakup and river fresh water flow to the Arctic Ocean is assessed.

2. INTAROS Data used in this report

Three different products from the INTAROS Data catalog have been used for the analyses described in the report (Table 1.). These cover different aspects of the ocean, sea ice and hydrology of the Arctic region. The first product (SMOS sea ice thickness) has been employed to guide the initialization strategy of a decadal prediction system with EC-Earth (Section 3); CERSAT sea ice concentrations was assimilated to generate the ICs of a seasonal prediction system with EC-Earth (Section 4); and the third product (Arctic-HYCOS river discharges) were assimilated to produce pan-Arctic hydrological analyses and forecast with the Arctic-HYPE model (Section)

Table 1. Summary of INTAROS Data used

Product	Variable	Producer	Period covered	Spatial and temporal resolution
SMOS	Sea Ice thickness	ESA	1st 2010 to March 03, 2020	October 1st to April 30th, daily value
CERSAT	Sea Ice Concentration	IFREMER	1992 to 2018	Original data interpolated to ORCA1 grid (~1 deg) and monthly averaged.
Arctic-HYCOS	River discharge	Arctic-HYCOS	1979-2020	Daily values at 428 river gauging station locations.

3. Benefits of sea-ice thickness initialization for seasonal-to-decadal climate predictions (SMHI contribution)

3.1. Background and initialization approach

Decadal climate prediction is a subject of ongoing research even though first quasi-operational systems exist. The main challenge in this context is a proper initialization of the coupled climate system, that is setting the global climate model into a state that adequately represents the current real world's climate for the time of the respective forecast's start. The primary source of predictability on decadal timescales is commonly seen in the ocean. However, other components are of certain relevance, too, one of them being sea-ice. When it comes to the assimilation, that is the translation of the real world's climate state into a proper model representation as initial conditions for starting a decadal climate prediction, various more or less sophisticated approaches exist. In most of these approaches, sea-ice thickness is not directly considered (also related to imperfect observational data on sea-ice thickness, for which long gridded products are not available). Often only primary oceanic parameters such as temperature and salinity and maybe sea-ice concentration are treated explicitly during the assimilation procedure, and sea-ice thickness in the model is left to physically adjust to the variables that are observationally constrained.

In close collaboration with colleagues at the Danish Meteorological Institute (DMI; a synergy with the ARCPATH-project, funded by the Joint Nordic Initiative on Arctic Research) SMHI developed a method to directly account for sea-ice thickness as represented in ocean reanalysis products and set up a decadal climate prediction system employing this approach. The general circulation model in use is EC-Earth (v3.3.1.1), incorporating model components for the atmosphere (IFS

c36r4), the ocean (NEMO3.6), and sea-ice (LIM3). A special feature of LIM3 is that it is based on multiple sea-ice categories (five in our case) for a single grid cell of the model. Our initialization method is based on the following procedure: (i) calculating the observed anomaly of local sea-ice volume (SIV; product of sea-ice thickness and concentration) for a given grid-cell; (ii) distributing these SIV-anomalies into sub-grid contributions of the five categories to the total grid-cell anomaly of sea-ice concentration and thickness. The distribution from (single-category) observed values to five-category contributions is done based on a local non-linear weight-likelihood function that was derived from a multi-centennial control simulation with EC-Earth3.

Complementing the development of this sea-ice thickness initialization approach, we performed sensitivity studies, integrating decadal “hindcasts” (forecasts performed for periods in the past) to check the relative contribution and potential added value of initializing specific variables. Three different “systems” have been set up:

- AI0 employing initialization of ocean temperature and salinity only (sea-ice fields are taken from a transient uninitialized *historical*-experiment, hence contain only the response to external forcing but no direct information about actually observed sea-ice variability)
- AI1 employing initialization of ocean temperature and salinity as well as sea-ice concentration (sea-ice thickness only indirectly constrained)
- AI2 employing initialization of ocean temperature and salinity as well as sea-ice concentration and thickness

For all three systems, 5-member ensembles have been initialized every 1 November 1979-2018 and integrated for 10 years and 2 months. “Observational” data used for initializing ocean and sea-ice fields is taken from ECMWF’s ORAS5 ocean reanalysis. For all fields and systems an anomaly initialization approach is used, that means the observational anomalies (compared to the climatological period 1979-2014) are added to the model’s climatology. This approach usually prevents substantial initialization shocks and subsequent model drifts. Atmospheric fields have been initialized from ERA-Interim reanalysis data.

To assess the general benefit from initialization, the prediction systems are additionally compared to results of a 5-member ensemble of transient *historical*-simulations (referred to as *FREE* in the following) that are “uninitialized”, that means they contain no direct information about any observed climate parameters only the response to external forcing such as concentrations of greenhouse gases and aerosols.

3.2. Results

The skill of these systems is assessed and compared among each other based on different metrics such as the Root Mean Square Error (RMSE) and the respective Skill Score (RMSESS). The latter simply quantifies the relative RMSE-reduction achieved by a forecast system compared to a specific reference forecast.

An example of our evaluations is given in Figure 3.1, showing the RMSE of the *FREE*-ensemble (top row) as well as the RMSESS of AI2 for the first predicted winter (DJF, actually reflecting a seasonal forecast) when compared to *FREE* (row 2), AI0 (row 3), and AI1 (row4), respectively, for sea-ice concentration (left), sea-ice thickness (center), and surface air temperature (right). The evaluations presented here are based on 20 start dates, to predict the winters 1996/1997-2015/2016.

It is clearly evident that AI2’s initialization of sea-ice thickness improves substantially the prediction of the sea-ice thickness itself. This is intuitive. The skill regarding predicted sea-ice concentrations is also predominantly higher even when compared to AI1 (including the initialization of sea-ice concentration), however, there are a few regions where the AI2-predictions are worse than AI1,

AI0, and even compared to FREE. The reasons for this are not entirely clear yet but at least partially explained by sampling uncertainty (only 20 predictions of 5 ensemble members each). Further in-depth analysis is necessary to understand the implications for predictive skill with respect to surface air-temperature. Fig. 3.1 shows (right column) in this respect that the initialization of sea-ice thickness leads to rather mixed results. While a positive impact is evident for large parts of North America, the North Atlantic, and Europe, AI2-predictions for Northeastern Asia, the Bering Sea, as well as the entire Arctic - that is the area where the most pronounced and direct effect of sea-ice thickness initialization was expected - are actually worse than FREE.

Still the overall conclusion is that AI2 yields the best predictions for the seasonal timescale shown here but also for multi-annual means predicted with longer lead-times. A respective scientific publication is currently in preparation (Tian et al.: Sensitivity of Arctic decadal predictions to sea-ice thickness initialization in EC-Earth3). For this reason, the AI2-approach, that is the anomaly initialization approach including sea-ice concentrations and sea-ice thickness was chosen to be used for a larger and more comprehensive set of decadal hindcasts and forecasts. A respective decadal prediction system has been set up by SMHI and DMI, consisting of 15 ensemble members in total and initialized annually on 1 November throughout the period 1960-2019. This decadal prediction system is currently run quasi-operationally, participating in the international exchange of annual-to-decadal climate predictions led and coordinated by the UK MetOffice (<https://hadleyserver.metoffice.gov.uk/wmolc/>) and contributing to CMIP6-DCPP. Additionally, it will state the baseline for further studies to be conducted within INTAROS, testing in how far the inclusion of new (INTAROS-produced) observational datasets for initialization may be able to improve our decadal predictions (SMHI-contribution to deliverable D6.11 due M58).

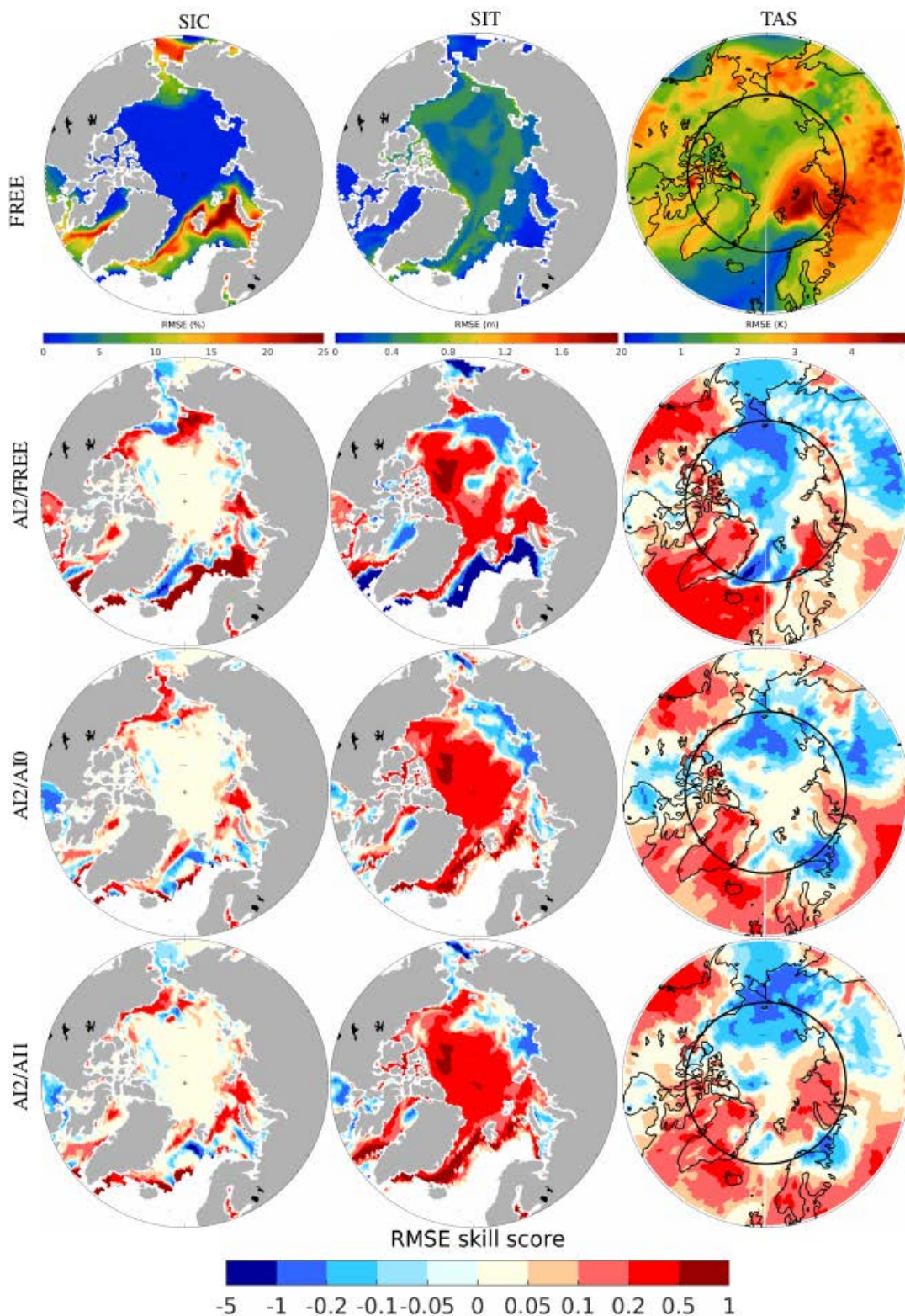


Figure 3.1. RMSE (top row) and RMSESS (row 2-4) for 20 (1996/1997 until 2015/2016) winter 1 prediction, comparing AI2 vs. FREE (row 2), AI2 vs. AI0 (row 3), and AI2 vs. AI1 (row 4), respectively, for sea-ice concentration (left), sea-ice thickness (center), and surface air temperature (right).

4. Impact of sea ice concentration assimilation in seasonal prediction biases (BSC contribution)

The previous section documented the benefits of initializing key sea ice variables, such as concentration and thickness, on the prediction skill at seasonal and longer timescales. This section assesses the added value of directly assimilating an INTAROS product (i.e. CERSAT sea ice concentrations; SIC) to initialize a seasonal hindcast with the same version of EC-Earth (Acosta Navarro et al., in preparation). Another seasonal hindcast with no SIC assimilation is also analyzed and acts as a baseline. Both sets of hindcasts are initialized every 1st of May and November for the period 1992-2018 with the same initial conditions for the atmosphere (directly from ERA5), but their respective ocean and sea ice are initialized differently, to make sure that they are consistent with each other (i.e. the ocean and the sea ice). Hindcasts NO-SIC (Table 4.1) uses sea ice and ocean initial conditions from an ocean-sea ice reconstruction in which only ocean temperature and salinity are restored to ORAS5 values, both at the surface and below the mixed layer (See Table 4.1 for additional details). The second hindcasts, CERSAT-SIC uses an identical protocol as NO-SIC, except that the sea ice concentration is restored to CERSAT values using heat flux adjustment in the sea ice model within the ocean-sea ice reconstruction providing initial conditions for the ocean and the sea ice (Table 4.1).

Hindcasts	Model	Atmosphere initial conditions	Ocean initial conditions	Restoring timescales
NO-SIC May 1st and Nov 1st initializations 1992-2018 10 members	EC-Earth3.3.1.1 NEMO3.6 - LIM3 - IFS c36r4 - H-Tessel	ERA5 (interpolated)	NEMO3.6-LIM3 reconstruction forced by ERA5 surface fluxes, restoring T and S.	Surface T and S: ~ 10 days. Subsurface T and S: ~ 3 days below mixed layer decreasing with depth.
CERSAT-SIC May 1st and Nov 1st initializations 1992-2018 10 members	EC-Earth3.3.1.1 NEMO3.6 - LIM3 - IFS c36r4 - H-Tessel	ERA5 (interpolated)	NEMO3.6-LIM3 reconstruction forced by ERA5 surface fluxes, restoring T, S and SIC	Surface T and S: ~ 10 days. Subsurface T and S: ~ 3 days below mixed layer decreasing with depth. SIC: ~3 days

Table 4.1: EC-Earth3.3 forecasts system description.

For the evaluation of the hindcasts, sea ice concentration and surface air temperature (TAS) mean biases were computed to estimate ensemble hindcast mean deviation from the observed climatology and deviation from the observed interannual variability, respectively. The evaluation is done for the first forecast month and aggregated months 2-4. Since the main goal was to

estimate model improvements from SIC assimilation exclusively, more sophisticated bias correction and/or calibration techniques were discarded to correct the raw hindcasts.

4.1. Summer hindcasts (May initialization)

Figure 4.1 shows the mean May SIC bias (vs. CERSAT) in NO-SIC (left), CERSAT-SIC (middle) and their mean absolute difference (right). Overall, there are relatively small SIC biases in both hindcasts, located over the marginal Seas, and there is an important bias reduction (over 30%) in the Seas of Labrador and Greenland when SIC is assimilated. SIC assimilation in May initializations reduces mean bias in the hindcasts. The bias in the summer (JJA) is large and negative (well over 30% in many regions) for both hindcasts and the impact of SIC assimilation is mostly lost by then (Figure 4.1), however there is an overall reduction (up to 3%) of RMSE in most of the Arctic when SIC is assimilated (not shown), which could be related to better representation of the sea ice thickness as it can be indirectly constrained by the assimilation.

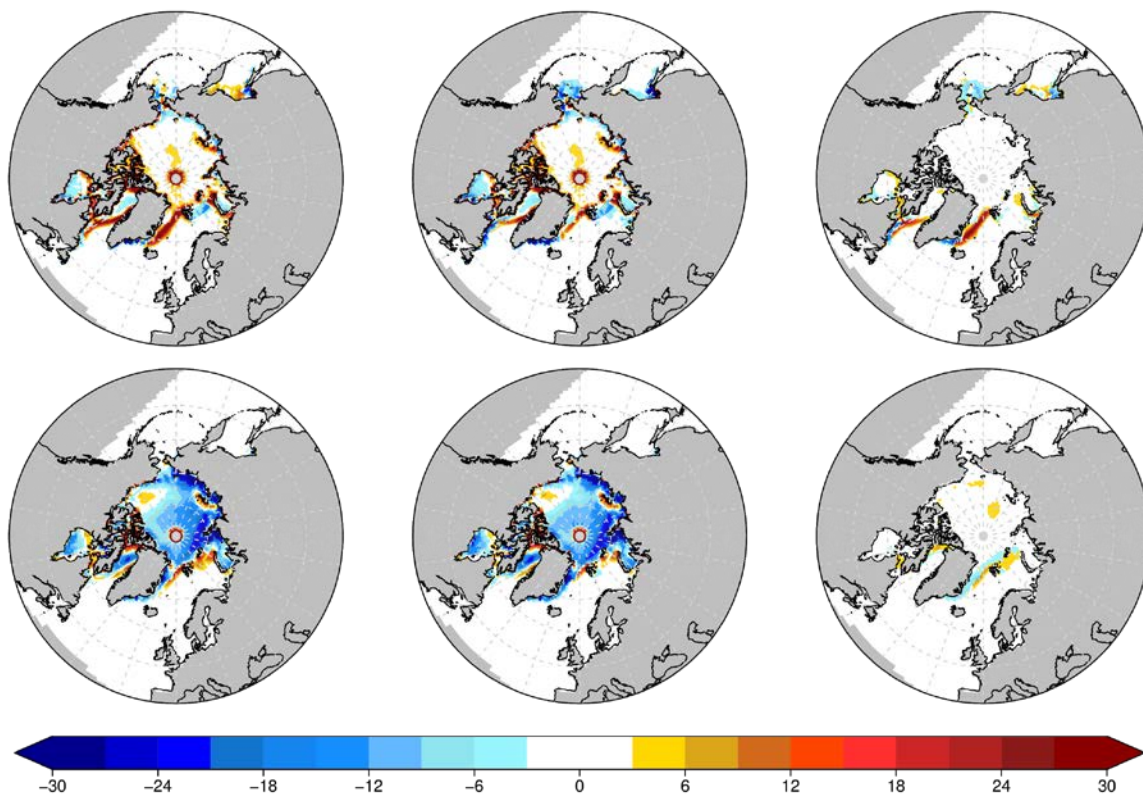


Figure 4.1: Ensemble mean May SIC bias in NO-SIC (top left), CERSAT-SIC (top middle) and their mean absolute difference (top right). Reference CERSAT SIC. Ensemble mean JJA SIC bias in NO-SIC (bottom left), CERSAT-SIC (bottom middle) and their mean absolute difference (bottom right). Reference CERSAT SIC.

Air temperature at 2 meters (TAS) bias in May (evaluated vs ERA5) displays a consistent pattern with SIC bias over Greenland Sea (Figures 4.2 and 4.1) showing larger positive SIC cover bias and a larger negative TAS bias in NO-SIC than in CERSAT-SIC, meaning that SIC assimilation improves the forecast system's negative bias by up to 1.4 K. There is a consistent and statistically significant reduction in May RMSE of TAS anomalies (not shown) in the Greenland Sea (up to 0.4 K) as a result of SIC assimilation at initialization, confirming an added value of SIC assimilation for improving mean state and variability in May hindcasts in the first forecast month. The analysis also suggests that SIC assimilation leads to a slight degradation ($\sim 0.3K$) on JJA TAS bias in the

Baffin Bay, Labrador, Barents and Kara Seas, showing larger positive bias in CERSAT-SIC than in NO-SIC.

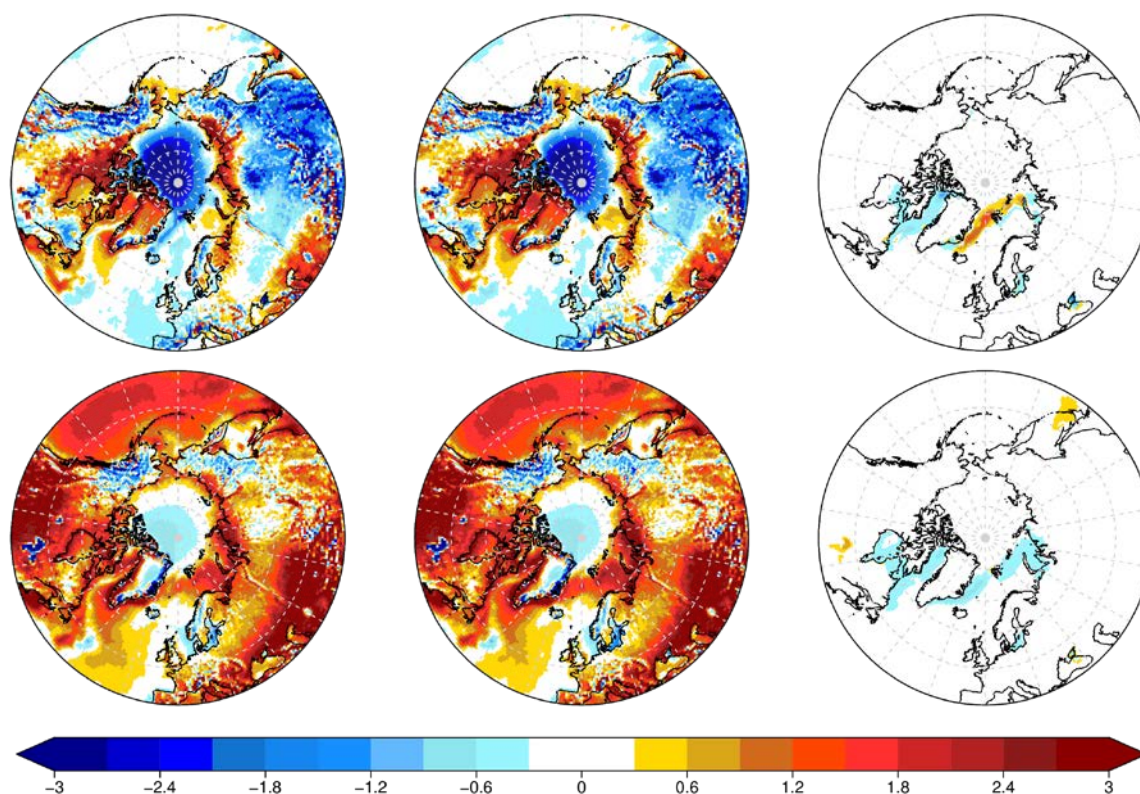


Figure 4.2: Ensemble mean May TAS bias in NO-SIC (top left), CERSAT-SIC (top middle) and their mean absolute difference (top right). Reference ERA5 TAS. Ensemble mean JJA TAS bias in NO-SIC (bottom left), CERSAT-SIC (bottom middle) and their mean absolute difference (bottom right). Reference ERA5 TAS.

4.2. Winter hindcasts (November initialization)

November SIC bias is overall positive in both CERSAT-SIC and NO-SIC hindcasts in most of the Arctic, but the assimilation results in an important reduction of SIC absolute bias in the Barents and Kara Seas and the Canadian Arctic of above 30% (Figure 4.3). Additionally, and in contrast with the results for the summer forecasts, SIC assimilation leads to reduced absolute mean bias throughout the winter (DJF), with the most consistent decrease over the Atlantic sector of the Arctic and the Okhotsk Sea.

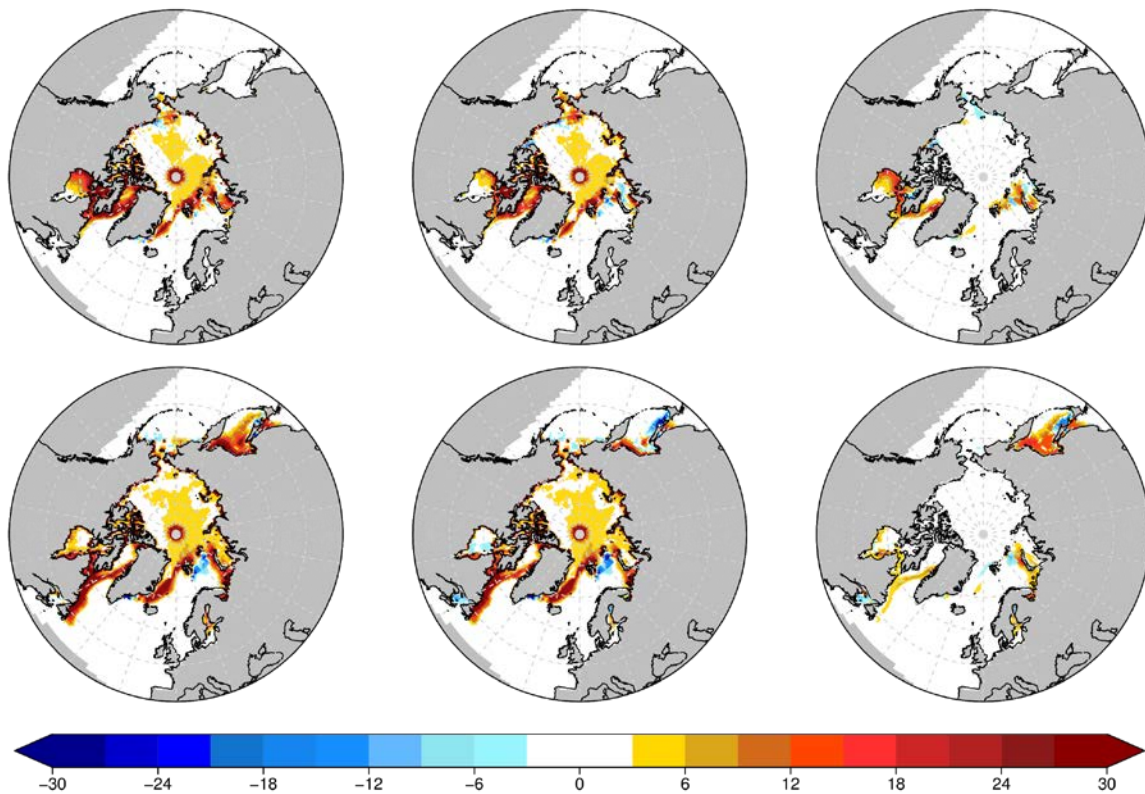


Figure 4.3: Ensemble mean November SIC bias in NO-SIC (top left), CERSAT-SIC (top middle) and their mean absolute difference (top right). Reference CERSAT SIC. Ensemble mean DJF SIC bias in NO-SIC (bottom left), CERSAT-SIC (bottom middle) and their mean absolute difference (bottom right). Reference CERSAT SIC.

November TAS absolute bias is largely reduced (up to 2 K) in most Arctic marginal seas due to the assimilation of SIC (Figure 4.4). This improvement in TAS persists well until DJF in most regions giving the hindcasts with SIC assimilation and added value in the early winter. Indeed, the assimilation reduces DJF TAS biases over the Canadian Arctic, Scandinavia, western Russia and parts of Okhotsk Sea and increases it over parts of Eurasia. Future work in INTAROS will involve extending the analysis to other variables (such as precipitation and SLP) and exploring the impact of this initialization to the predictive skill.

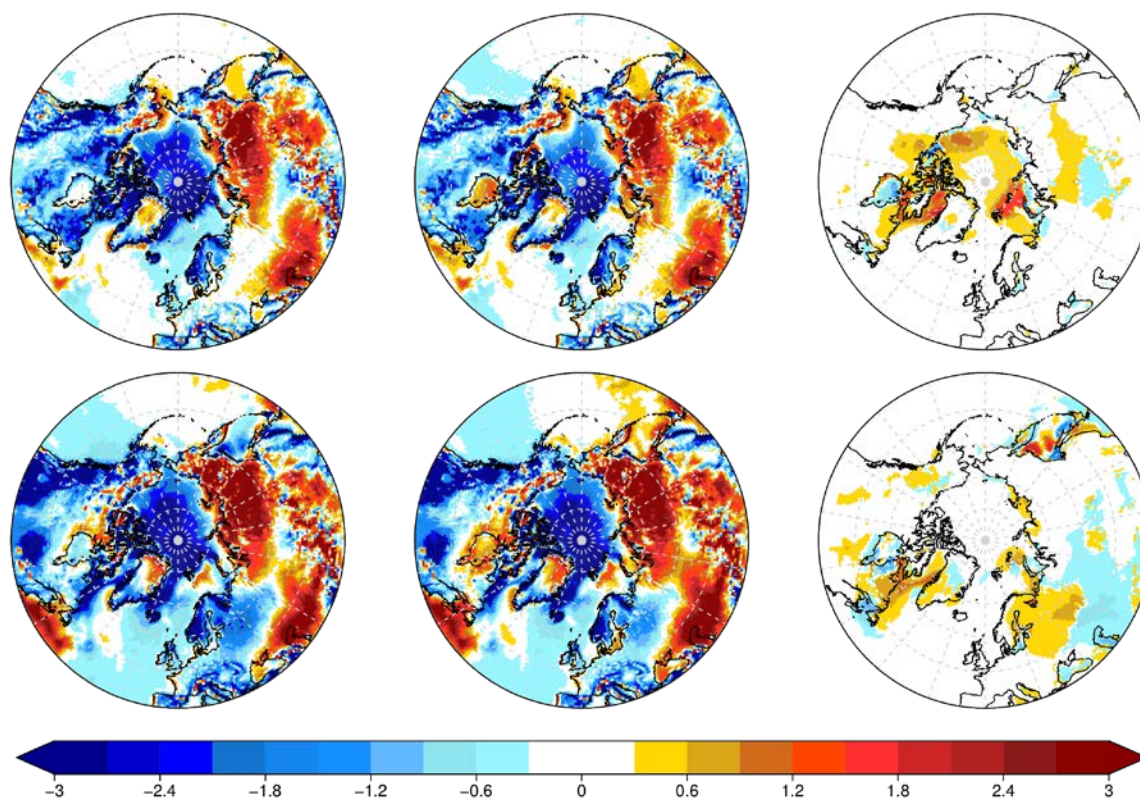


Figure 4.4: Ensemble mean November TAS bias in NO-SIC (top left), CERSAT-SIC (top middle) and their mean absolute difference (top right). Reference ERA5 TAS. Ensemble mean DJF TAS bias in NO-SIC (bottom left), CERSAT-SIC (bottom middle) and their mean absolute difference (bottom right). Reference ERA5 TAS.

5. Impact of Ocean and Sea Ice Initialisation On Seasonal Prediction Skill in the Arctic (NERSC contribution)

5.1. Seasonal to decadal predictions of regional Arctic sea ice by assimilating sea surface temperature in the Norwegian Climate Prediction Model

The version of the Norwegian Climate Prediction Model (NorCPM) that only assimilates anomaly of sea surface temperature (SST from HadISST2) with the Ensemble Kalman Filter (and 30 members) has been used to investigate the seasonal to decadal prediction skill of regional Arctic sea ice extent (SIE). The prediction skill is assessed based on a suite of NorCPM retrospective predictions. The seasonal hindcasts are for the period 1980 to 2010 with 4 start dates per year and 9 members run for 1 year each. The decadal hindcasts are tested from 1950-2010 with a hindcast started every 2 years and 20 members. We show that decadal prediction of sea ice extent has no skill beyond 1 year lead time (Figure 5.1). Seasonal prediction of pan-Arctic SIE is skillful at lead times up to 12 months, which outperforms the anomaly persistence forecast. The SIE skill varies seasonally and regionally. Among the five Arctic marginal seas, the Barents Sea has the highest SIE prediction skill, which is up to 10–11 lead months for winter target months. In the Barents Sea, the skill during summer is largely controlled by the variability of solar heat flux and

the skill during winter is mostly constrained by the upper ocean heat content/SST and also related to the heat transport through the Barents Sea Opening. Compared with several state-of-the-art dynamical prediction systems, NorCPM has comparable regional SIE skill in winter due to the improved upper ocean heat content (Dai et al., 2020). The relatively low skill of summer SIE in NorCPM suggests that SST anomalies are not sufficient to constrain summer SIE variability and further assimilation of sea ice thickness or atmospheric data is expected to increase the skill

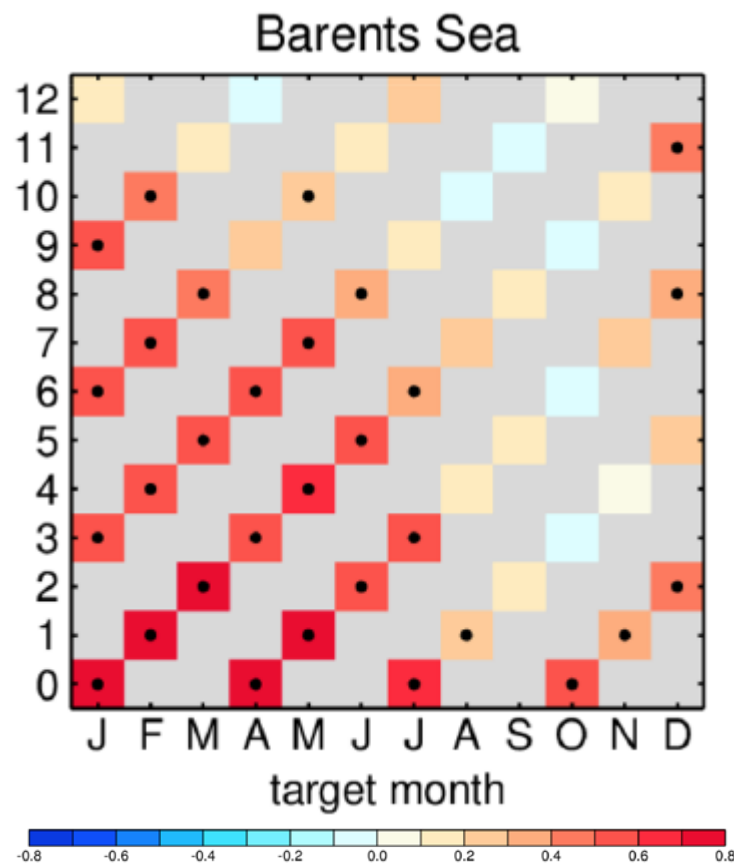


Figure 5.1: Anomaly correlation coefficient of detrend sea ice extent in the Barents Sea of the NorCPM hindcasts with observation organised as a function of target month (x-axis) and lead months (y axis). Dots indicate that ACC are statistically significant at 95% confidence level. Gray shading is used when hindcasts are not available.

5.2. Impact of Ocean and Sea Ice Initialisation On Seasonal Prediction Skill in the Arctic

In order to further enhance the skill of seasonal prediction we have decided to make use of sea ice concentration that is widely available since the 80s and allows us to assess robustly its impact for seasonal prediction. In Kimmritz et al 2019, we have used an idealised twin experiment to identify the optimal manner to assimilate sea ice concentration in NorCPM. It was shown that using strongly coupled data assimilation of ocean and sea ice (meaning that sea ice observations are used to update both the sea ice and ocean components) are performing better than weakly coupled data assimilation (meaning that sea ice data only updates the sea ice component) because the dynamical consistency is improved and we use the observations more efficiently. We

also show that updating the multi-category sea ice concentrations from the aggregated concentrations yields very large improvements in sea ice thickness which are of critical importance for seasonal to interannual predictions. We have also tested this implementation in a real-time framework with the Norwegian Climate Prediction Model, to our knowledge the first attempt with a climate prediction system using strongly coupled data assimilation of ocean and sea ice. We are assimilating anomalies of SST from HadISST2, hydrographic profiles from EN4 and sea ice concentrations from HadISST2. We have decided to use this data set instead of CERSAT to ensure consistency of the SST and ice concentration products. We assess the seasonal prediction skill of this version for the period 1985 to 2010 with 4 start dates per year, 9 members and forecast length of 1 year each, running two sets: one started from a reanalysis with ocean data only and one assimilating ocean and sea ice. The reanalysis that assimilates just ocean data exhibits skillful hydrography in the upper Arctic Ocean and features an improved sea ice state, such as improved summer SIC in the Barents Sea, or reduced biases in sea ice thickness. Additional DA of SIC data notably further corrects the initial sea ice state, confirming the applicability of the results of Kimmritz et al. (2019) in a historical setting. The resulting prediction skill of SIE is widely enhanced by assimilation of sea ice concentration compared to the system assimilating only ocean data (Figure 5.2). Particularly high skill is found for July-initialized autumn SIE predictions.

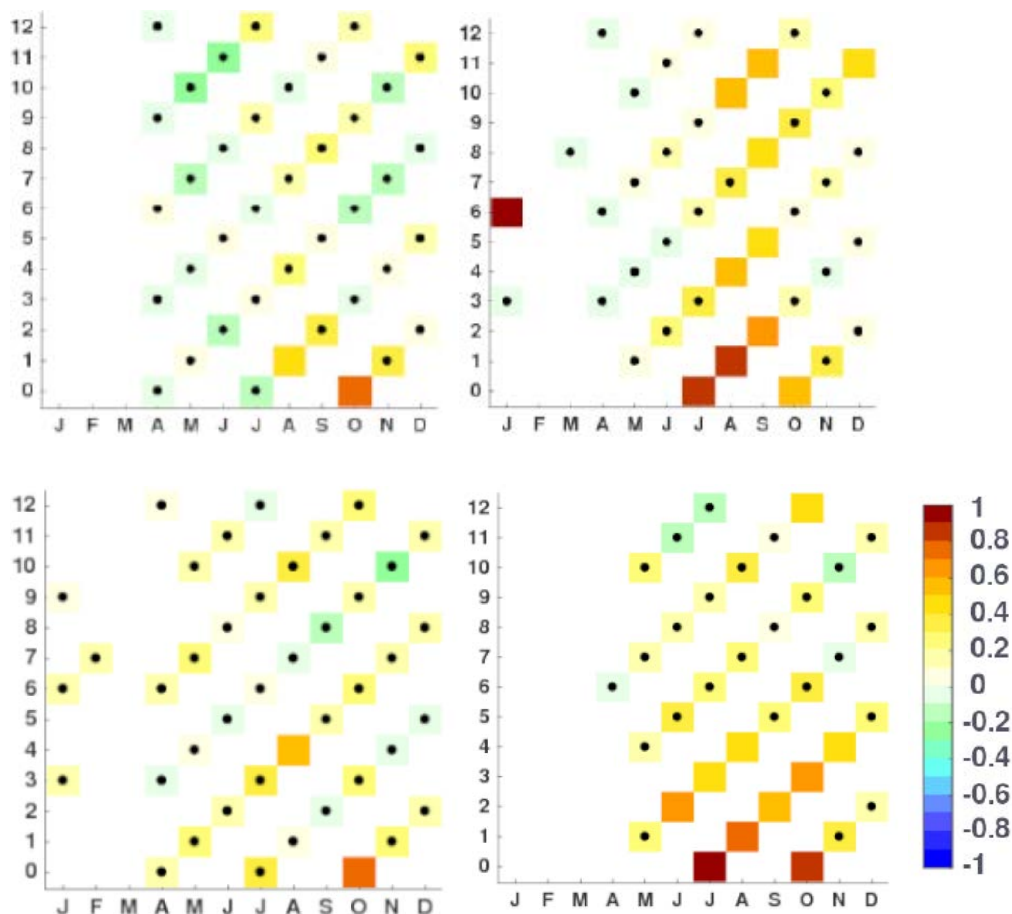


Figure 5.2: Anomaly correlation coefficient of detrended sea ice extent in the Kara Sea (first line) and Chukchi Sea (second line) of the NorCPM hindcasts with observation organised as a function of target month (x-axis) and lead months (y axis). Dots indicate that ACC are not statistically significant at 95% confidence level. On the left we see the prediction in the system assimilation only ocean data while it assimilates ocean and sea ice on the right.

Ongoing and Future work:

We are currently testing the benefit of further assimilating sea ice thickness from a Merged product of ENVISAT and CRYOSAT2 ice thickness for the period 2003-2011 and for a merged product of CRYOSAT2+SMOS (a product called C2SMOS and included in the INTAROS portfolio) for the period 2011-2020. We will in particular assess the added value of that product for prediction of sea ice extent. Simulations are ongoing.

6. Impact of hydrological observations on prediction of spring floods, river ice breakup and freshwater flow to Arctic Ocean (SMHI contribution)

The aim of this activity is to demonstrate the added value of the integrated arctic observation systems (iAOS) for enhancing and making available hydrological model predictions for the major Arctic rivers. The main objective is to combine the river discharge data from the Arctic Hydrological Cycle Observing system (Arctic-HYCOS) - that was assessed and enhanced in INTAROS WP2 – with the pan-arctic hydrological model Arctic-HYPE provided by SMHI (<http://hypeweb.smhi.se>), to predict and monitor fresh water inflow to the Arctic Ocean and changes in Arctic hydrological regimes. The demonstration case consists of an operational application of the Arctic-HYPE model providing daily analyses of the last 60 days, and medium range forecast of the coming 10 days. The Arctic-HYPE analyses and forecasts are stored at SMHI open data repositories and will be made available using OPeNDAP server technology. Arctic-HYCOS observations are accessed by the operational service using the tools and metadata provided by INTAROS WP2 catalogue (<https://catalog-intaros.nersc.no/dataset/arctic-hycos-hydrological-data/>). One of the goals is to demonstrate the improvement of the pan-arctic hydrological analyses and forecasts by assimilating the river discharge data in the operational Arctic-HYPE application. A second goal is to demonstrate the ability to build user-tailored data products based on the Arctic-HYPE data accessed through an OPeNDAP server. The latter will be illustrated by a use-case in Republic of Sacha (Yakutia), in Far-East Russia, where a subset of the Arctic-HYPE model is used for spring flood and river ice breakup forecasting in the major Yakutia rivers.

6.1. Pan-arctic hydrological model Arctic-HYPE

Arctic-HYPE version 4.2 is a new pan-arctic application of the hydrological model HYPE (Hydrological Predictions for the Environment; Lindström et al. 2010; SMHI <http://hypeweb.smhi.se>) simulating water balance of glaciers, snow, soil, lakes and rivers, representing processes such as runoff, river discharge and water level, and river ice growth, melt and breakup. It is based on Arctic-HYPE version 3.1 which was previously applied to the Lena river basin (Gelfan et al, 2017) and the Hudson Bay complex (MacDonald et al, 2018). The model domain covers the land areas draining into the Arctic Ocean and related water bodies in the northern seas as defined in Figure 6.1. The total model area is 26 Mkm² distributed on 34421 sub-basins with a median area of 623 km². Main improvements compared to Arctic-HYPE v3.1 are a) improved sub-basin delineation based on the World-wide HYPE (Arheimer et al, 2020) with further adjustments to the Arctic-HYCOS station locations, b) a new parameterization of frozen soil impact on runoff generation, c) overall improved calibration of water balance and cryospheric processes including evaporation, snow, and river ice using primarily local observations from Yakutia river gauges and research basins. Daily forecasts for the next 10 days are produced with meteorological forcing data from the ECMWF deterministic medium range weather forecasts. The forecast model is initialized by an analysis of the previous 60 days, forced by the HydroGFD v3 temperature and precipitation data (Berg et al, 2017), in which the Arctic-HYCOS data will be assimilated to improve the initialization. The historical simulations include daily river discharge for the period 1979 to 2019.

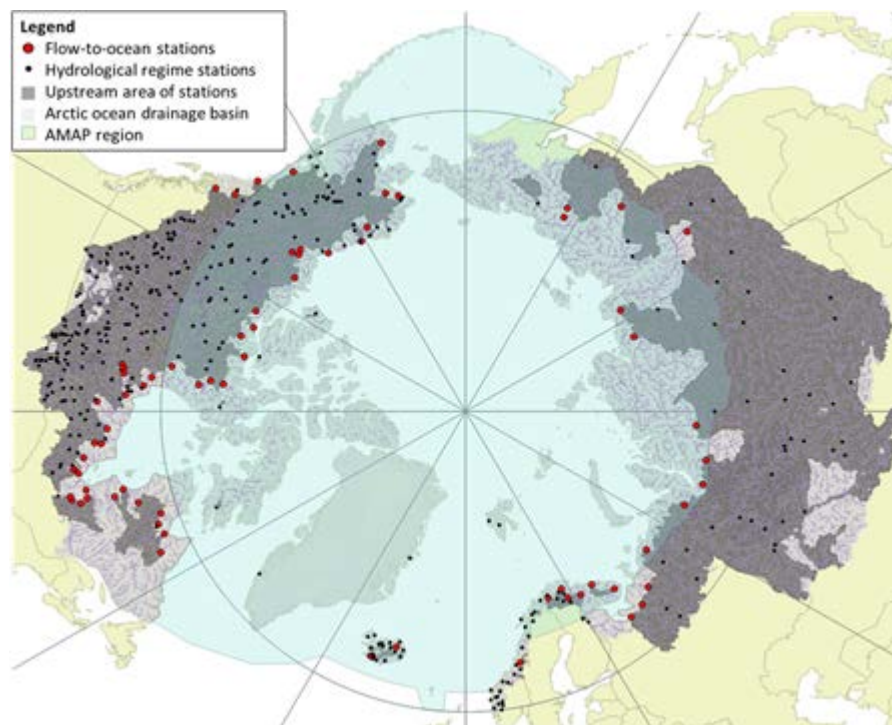


Figure 6.1 Drainage basin of the Arctic Ocean and related water bodies in the northern seas as represented in the Arctic-HYPE model (light grey), the location of the Arctic-HYCOS stations and their upstream drainage basins (dark grey).

6.2. Arctic-HYPE v4.2 OPenDAP data service

The previous version of the Arctic-HYPE model (v3.1) was disseminated through an interactive map browser service at <http://hypeweb.smhi.se>. Users could download data from one sub-basin at the time by selecting the location in the web map interface. All data were openly available; however, the limitation of data access through the interactive map browser prevented structured data access, access of larger parts of the model domain. Data from the full model domain was available for licensed users, but only through a FTP server, with the backside that users had to download data from the full data domain before extracting their sub-domain of interest.

To improve the Arctic-HYPE data access, and to open up for structured retrieval through the iAOS, a new data dissemination service has been developed using a THREDDS data server implementing the OPenDAP protocol. The server will be hosted at www.smhi.se providing Arctic-HYPE data in NETCDF format following the CF-convention (<http://cfconventions.org/>).

6.3. Yakutia spring flood and river ice breakup forecasting

A sub-set of the Arctic-HYPE model covering the Republic of Sacha (Yakutia) in Far East Russia, was used to develop a spring flood and river ice breakup forecasting service (Figure 6.2). This use-case is developed in collaboration with the HYPE-ERAS and Hydrology TEP, funded through a Belmont Forum Arctic II collaborative research action and the European Space Agency, respectively. For the spring flood 2020, the new version of Arctic-HYPE (v4.2) was implemented to run operationally in the SMHI production system, publishing the outputs of the 10 day forecast and 60 day analysis daily in an internal offline version of the OPeNDAP server. Results were extracted for selected locations in the Yakutia domain as exemplified in Figure 6.3, which shows the forecast issued 2020-05-08 for the Lena River at Kangalassy, just upstream of the city of Yakutsk. Similar forecast plots were produced for about 90 points of interest (Figure 6.2). The forecast points were selected based on availability of in-situ observation as well as stakeholder interest. A summary of the forecasts providing information on the expected river ice breakup dates, and river water level tendencies were made every day by collaborators at the Melnikov Permafrost Institute in Yakutsk, and communicated with the local stakeholders. The 2020 river ice breakup in the Lena river at Yakutsk took place on the 11th of May, which was correctly predicted by the Arctic-HYPE forecast issued on the 8th of May (Figure 6.3). A few days after the on-set of ice flow in the river, an ice jam developed in the Lena river at Kangalassy; downstream of Yakutsk; with flooding of parts of the city.

This use-case illustrates how the Arctic-HYPE data may be used in a future application when it is made available in the open OPeNDAP server. It should also be noted that in this example, observations of water level and river ice conditions from Roshydromet were collected in collaboration with local stakeholders and used for verification of the hindcast model results. River ice, water level and river discharge data set from historical period 2008-2017 were used to establish first of all stage-discharge relationships to transform the discharge simulated by the model to water level predictions, and secondly long-term statistics on most efficient river ice porosity trigger break up and ice flow conditions (Figure 6.3). These data are not part of the iAOS, but the use-case illustrates the situation where a local user can combine the open available data provided by the iAOS with their own data to produce enhanced forecasting products.

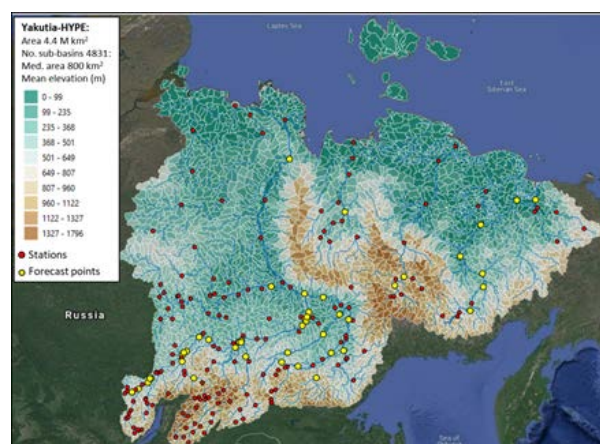


Figure 6.2 Map of Yakutia-HYPE sub-domain of the Arctic-HYPE model, local station network, and forecast points.

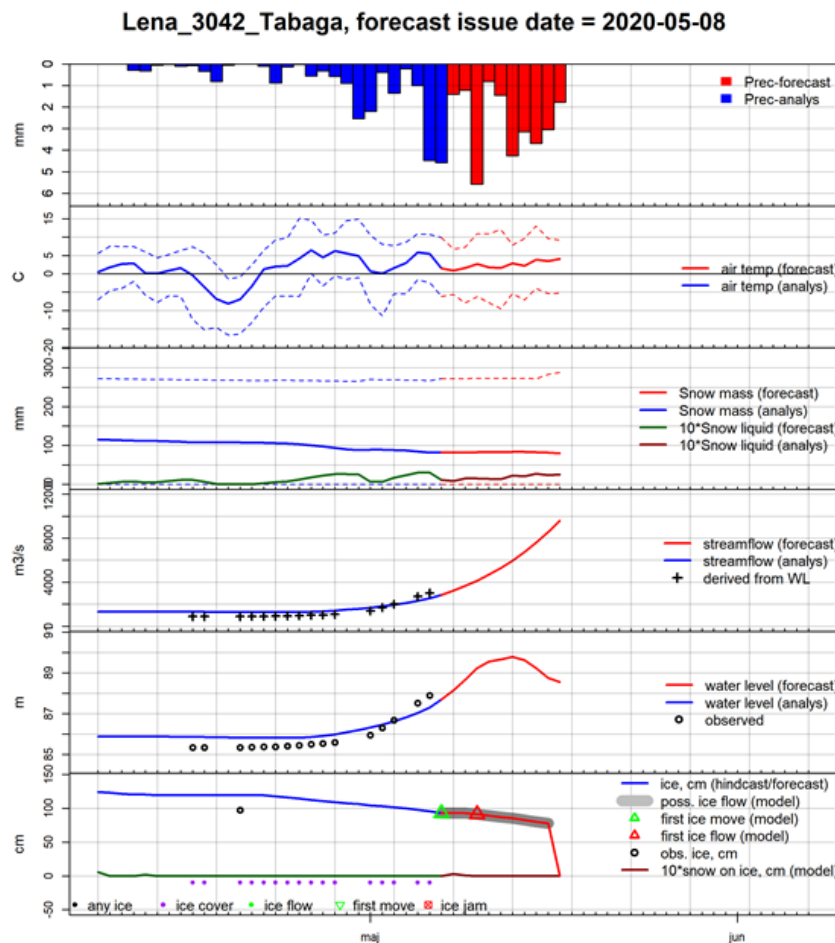


Figure 6.3 Arctic-HYPE forecast for Lena river at Tabaga (upstream of the city of Yakutsk), forecast issue date 2020-05-08. Hindcast and available observations (blue lines and symbols) and forecast (red lines and symbols), from the top, 1) precipitation in the upstream area (mm), 2) mean temperature (dotted lines indicate minimum and maximum), 3) snow water equivalent (mm), 4) river discharge (m³/s), 5th panel: river water level (m), 6th panel: ice thickness (cm) and so-called ice-processes. The Tabaga station is part of the Arctic-HYCOS observation system which is part of iAOS.

7. Conclusions

The key outcomes of the report are summarised in the following:

- Evaluations of sensitivity studies regarding retrospective EC-Earth3-based climate forecasts (hindcasts) performed for the period 1996-2016 show that the initialization of sea-ice concentrations and in particular sea-ice thickness is in general beneficial for seasonal and decadal prediction skill over the Arctic region. The developed approach has been used for a quasi-operational decadal climate prediction system (joint effort of SMHI and DMI) participating in CMIP6-DCPP and in the international exchange of annual-to-decadal climate predictions (<https://hadleyserver.metoffice.gov.uk/wmolc/>). This system will state the baseline for further studies on the added value of new observational products provided by INTAROS for the initialization of decadal climate predictions. Assimilation of anomaly of sea ice concentration in NorCPM yields substantial improvement of sea ice thickness which allows the system to enhance seasonal prediction of sea ice extent.

- Two sets of EC-Earth-based May-initialized retrospective forecasts covering the period 1992-2018 have shown that assimilation of CERSAT SIC data has a positive effect in reducing mean SIC and TAS bias in the first month of the forecast. For lead times 1-3 months (JJA) the effect of SIC assimilation is mostly lost and in some regions may degrade forecast quality. With NorCPM it was shown that the skill during that period is mostly driven by atmospheric variability but that skill can be achieved by reducing error in the sea ice thickness and SIE during summer time can be predicted up to a year in the Kara Sea and up to 4 months in the Chukchi Sea. The SIC assimilation has a stronger effect in winter hindcasts showing larger improvements in the first forecast month, but also further into winter for both SIC and TAS in terms of bias. To assess whether SIC assimilation affects forecasts biases in neighbouring continental regions (via dynamical linkages), larger hindcasts (in terms of members) are required. Additionally, comparison against other observational products would help address whether observational uncertainty plays an important role in hindcast quality. For this reason larger ensembles are being produced in which not only CERSAT SIC is assimilated, but also EUMETSAT and ORAS5 SIC.
- The Arctic-HYPE model have been setup to interact with the integrated Arctic observations system; hydrological observations are collected from Arctic-HYCOS observation system for assimilation, and an OPeNDAP server have been developed to make Arctic-HYPE analyses and forecast data available for further exploitation. The potential benefit of the integrated observation and modelling system is demonstrated by the Yakutian spring flood and river ice breakup forecasting use case. The impact of assimilating the Arctic-HYCOS observations on predictions of freshwater flow to the Arctic Ocean and local streamflow forecasting will be further explored in future experiments.

Most of the results presented in this deliverable describe ongoing work, which will be finalized, and complemented with additional studies (in which, e.g., INTAROS sea ice thickness data is directly assimilated) in the final deliverable (D6.11), entitled “Climate model initialization: final report on the added value of using data from INTAROS”.

REFERENCES

Acosta Navarro J.C., Lapin V., Tourigny E., Sicardi V., Ruprich-Robert Y., Amaral-Ramos A. Echevarria P., Cruz-García R., Arsouze T., and Ortega P. (In preparation) Added value of Arctic sea ice concentration assimilation in seasonal forecasts with EC-Earth3.

Arheimer B. et al. (2020) Global catchment modelling using World-Wide HYPE (WWH), open data, and stepwise parameter estimation, *Hydrol. Earth Syst. Sci.*, 24, 535–559, <https://doi.org/10.5194/hess-24-535-2020>.

Berg, P., Donnelly, C., and Gustafsson, D.(2018). Near-real-time adjusted reanalysis forcing data for hydrology, *Hydrol. Earth Syst. Sci.*, 22, 989–1000, <https://doi.org/10.5194/hess-22-989-2018>.

Dai P.X., Gao Y.Q., Counillon F., Wang Y.G., Kimmritz M., Langehaug H. (2020) Seasonal and decadal predictions of regional Arctic sea ice by assimilating sea surface temperature in the

Norwegian Climate Prediction Model. *Climate Dynamics*, Published Online. <https://doi.org/10.1007/s00382-020-05196-4>.

Gelfan A. et al. (2017) Climate change impact on the water regime of two great Arctic rivers: modeling and uncertainty issues. *Climatic Change*, 141 (3): 499-515. doi:10.1007/s10584-016-1710-5. Number of citations: 42.

Kimmritz, M., Counillon, F., Smedsrud, L. H., Bethke, I., Keenlyside, N., Ogawa, F., & Wang, Y. (2019) Impact of ocean and sea ice initialisation on seasonal prediction skill in the Arctic. *Journal of Advances in Modeling Earth Systems*, 11. <https://doi.org/10.1029/2019MS001825>.

Lindström G. et al (2010). Development and test of the HYPE (Hydrological Predictions for the Environment) model – A water quality model for different spatial scales. *Hydrology Research* 41.3-4:295-319.

MacDonald M. K. et al. (2018). Impacts of 1.5 and 2.0 °C warming on pan-Arctic river discharge into the Hudson Bay Complex through 2070. *Geophysical Research Letters*, 45, 7561–7570. <https://doi.org/10.1029/2018GL079147>.

-- END OF DOCUMENT --



INTAROS

This report is made under the project
Integrated Arctic Observation System (INTAROS)
funded by the European Commission Horizon 2020 program
Grant Agreement no. 727890.



Project partners:

